

2014

Differential Spectral Imaging of the CN Violet Band in Laser-Induced Plasmas on TNT Simulant Molecules

J. Merten

Arkansas State University - Main Campus

M. Jones

Anton Paar

S. Hoke

Arkansas State University - Main Campus

S. Allen

Embry Riddle Aeronautical University, allens17@erau.edu

Follow this and additional works at: <https://commons.erau.edu/publication>



Part of the [Chemical Engineering Commons](#), and the [Physics Commons](#)

Scholarly Commons Citation

Merten, J., Jones, M., Hoke, S., & Allen, S. (2014). Differential Spectral Imaging of the CN Violet Band in Laser-Induced Plasmas on TNT Simulant Molecules. *Journal of Physics: Conference Series*, 548(). <https://doi.org/10.1088/1742-6596/548/1/012042>

This Article is brought to you for free and open access by Scholarly Commons. It has been accepted for inclusion in Publications by an authorized administrator of Scholarly Commons. For more information, please contact commons@erau.edu.

Differential Spectral Imaging of the CN Violet Band in Laser-Induced Plasmas on TNT Simulant Molecules

J Merten¹, M Jones, S Hoke¹ and S Allen³

¹Department of Chemistry and Physics, Arkansas State University, P.O. Box 419, State University, AR, 72467, USA

²Anton Paar, 15421 Vantage Parkway W., Houston, TX, 77032, USA

³Department of Mechanical Engineering, Embry Riddle Aeronautical University, 600 S. Clyde Morris Blvd., Daytona Beach, FL, 32114, USA

jmerten@astate.edu

Abstract. Dual channel emission imaging of m-nitrobenzoic acid and benzoic acid was performed in order to visualize the morphology of the CN violet band emission of a TNT analogue. The CN channel was corrected for continuum emission using a simultaneously imaged background channel. Simultaneous dual channel imaging alleviated problems with shot to shot variation in the plasma morphology due to the friable substrates and showed differences between plasmas formed on the two targets.

1. Introduction

Although LIBS is primarily an elemental technique, there have been attempts to use the plasma's molecular emission to identify complex molecules in the ablated sample. As such, the origin of diatomic emission from the LIBS plasma is relevant to any potential selectivity. Previous studies have suggested that C₂ and CN emission may arise from native CN bonds cleaved from molecular substrates, especially after 266nm or ultra-short pulse ablation [1]. Some researchers have suggested that the temporal development of the CN emission indicates the origin of the emitting molecules, with single exponential decays arising from native-cleaved CN bonds and more complex development indicating that the CN arises from reactions in the plasma. More recently, investigations of the morphology of the molecular and atomic emission from the plasma have suggested that the location of the emission in the plasma may carry information about the ablated target [2]. In order to better understand the origin of the CN emission following single laser shots on pressed pellets of a TNT analogue, we present differential spectral imaging of CN emission with simultaneous spectra after ablation of m-nitrobenzoic acid (NBA) and benzoic acid (BA). The former is used as a convenient analogue of TNT with the latter used as a control as it contains no native C-N bonds.

2. Instrument and data processing

The optical arrangement is summarized in Figure 1. The pressed pellet samples were ablated with 20 mJ of 355 nm emission provided by a Continuum Surelite. The spot diameter was approximately 500 μm at the target. LIBS plasma emission was collimated with an f=12.5 cm NUV achromat. A microscope slide picked off a portion of the collimated light for imaging onto the spectrometer slit. The remaining light was split into CN and background correction arms with a dichroic beamsplitter.



Spectral channels were isolated with interference filters. The slightly magnified (1.2x) images were collected simultaneously on the same ICCD face (Andor USB Istar, 2048x512). Simultaneous collection of signal and background images was necessary to minimize irreproducibility of plasma morphology caused by the friable pressed powder samples. Data were processed in Labview, correcting relative efficiencies of the two channels using the image of a fiber optic coupled to a standard deuterium lamp, while image positions (and rotation) were registered using the dual images of a geometric alignment grid. Figure 2 shows the relative spectral positions of the two channels. Because a narrow-band filter overlapping the CN band was not available, the CN channel integrates some atomic emission, particularly at early times.

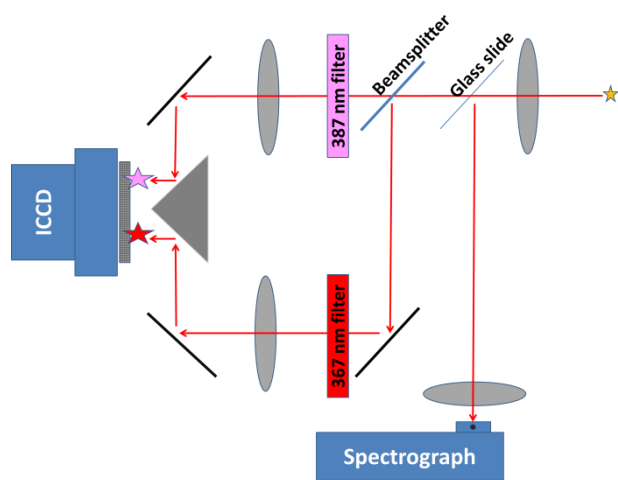


Figure 1. Optical arrangement used to acquire single-shot, dual-channel images with simultaneous spectra. The image at the spectrograph is rotated such that the plasma image propagates along the slit. The spectrum is integrated over the height of the plasma which is centered laterally on the slit.

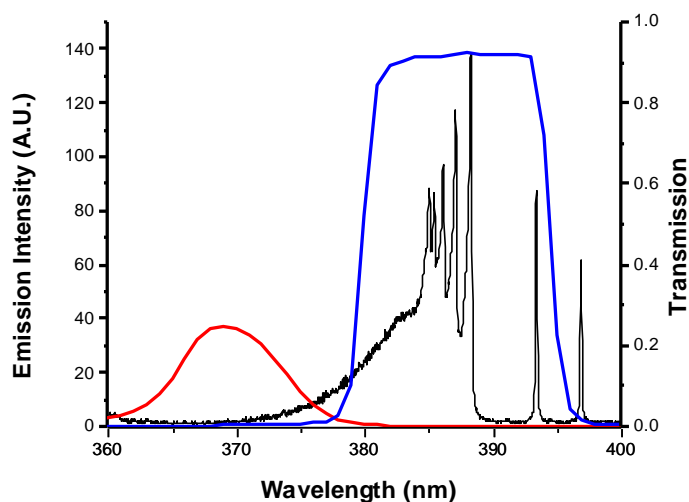


Figure 2. Position of CN ($\lambda_{\text{center}}=388$ nm) and background channel ($\lambda_{\text{center}}=370$ nm) relative to the CN violet band $\Delta v=0$ emission.

3. Imaging and conclusions

In both the BA and NBA plasmas, the imaging at the earliest time is prone to artifacts as the CN emission sits atop a substantial continuum, with additional structure at the long wavelength side of the CN band, see Figures 3 to 6. The net NBA image at 50 ns is of poor quality, though comparison with the 100 ns image suggests that the indicated net CN emission may be real. In the earliest BA image,

there is clear evidence of a symmetrical CN emission front near the presumed atmosphere/plasma interface, in contrast to the more irregular emission seen in the early NBA image.

The net CN imaging at later times is less prone to artifacts, with a decreased and less structured background. The net CN images on BA continue to show more of a dome shape, while the NBA emission remains more chevron-shaped and dense. Though the plasmas produced on the two substrates produce different image morphologies, it is not clear if this is a result of different chemistry in the plasma or simply physical/mechanical differences in the laser-target interaction and subsequent fluid flow.

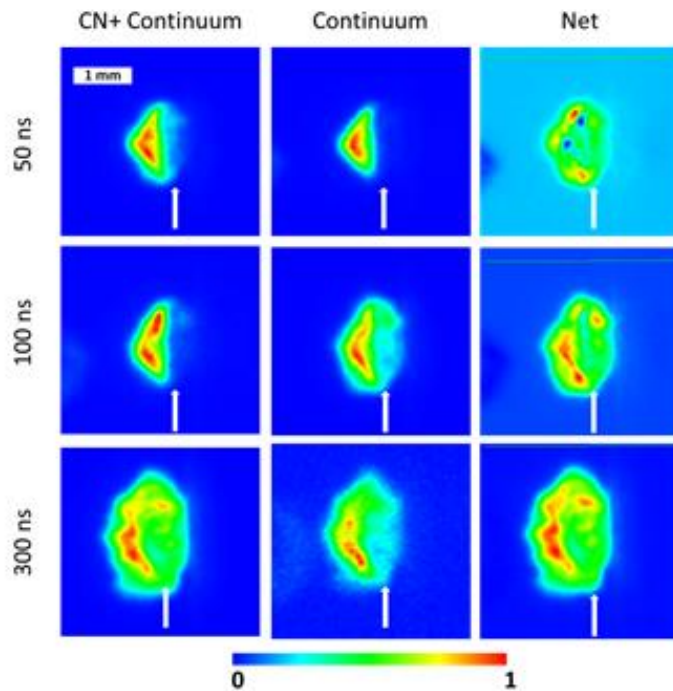


Figure 3. Nitrobenzoic acid imaging and spectra at indicated delays. The plasma propagates from right to left with time. The laser is incident from the image left. Each image is scaled separately such that absolute comparisons are not possible. The arrow indicates the approximate location of the sample surface. Gate widths are 50, 100, and 200 ns, respectively, from early to late.

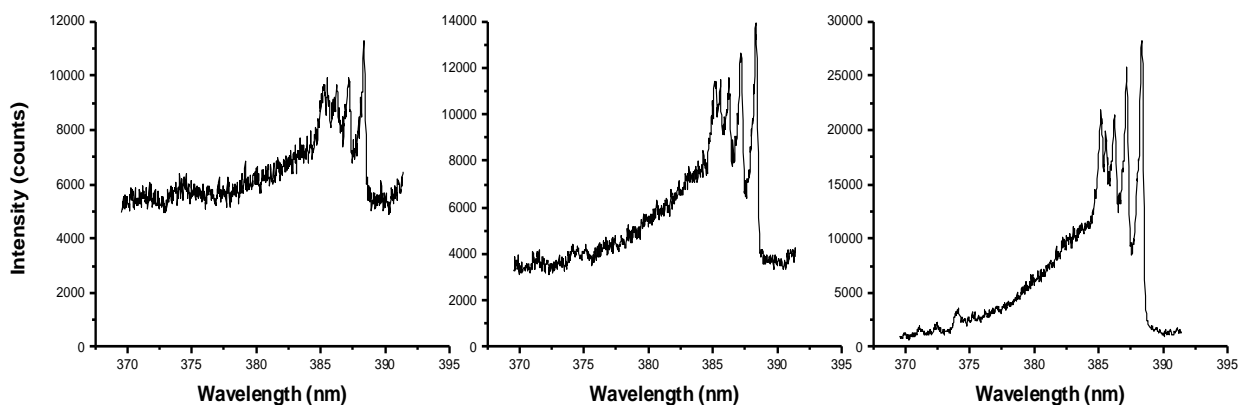


Figure 4. Nitrobenzoic acid CN emission spectra collected simultaneously with images in Figure 3. Gate positions and widths are as in Fig. 3.

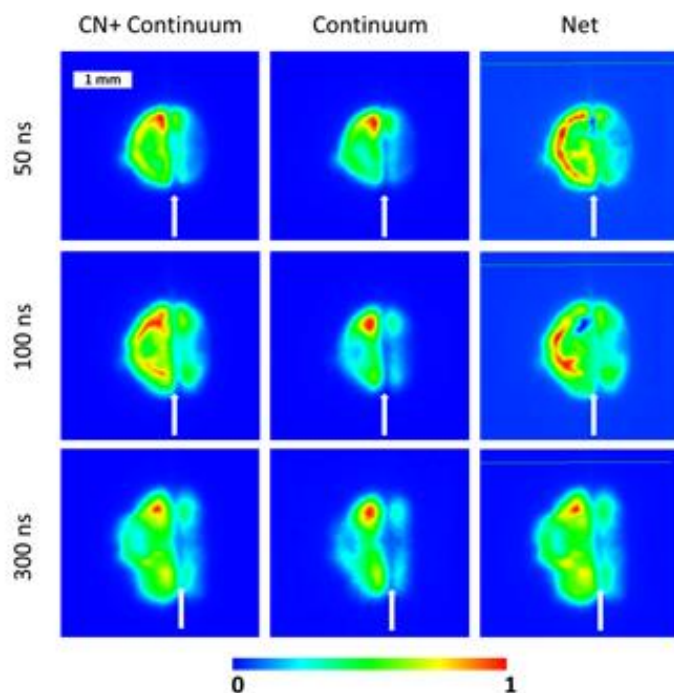


Figure 5. Benzoic acid imaging and spectra at indicated delays. The plasma propagates from right to left with time. The laser is incident from the image left. Each image is scaled separately such that absolute comparisons are not possible. The arrow indicates the approximate location of the sample surface. Gate widths are 50, 100, and 200 ns from early to late.

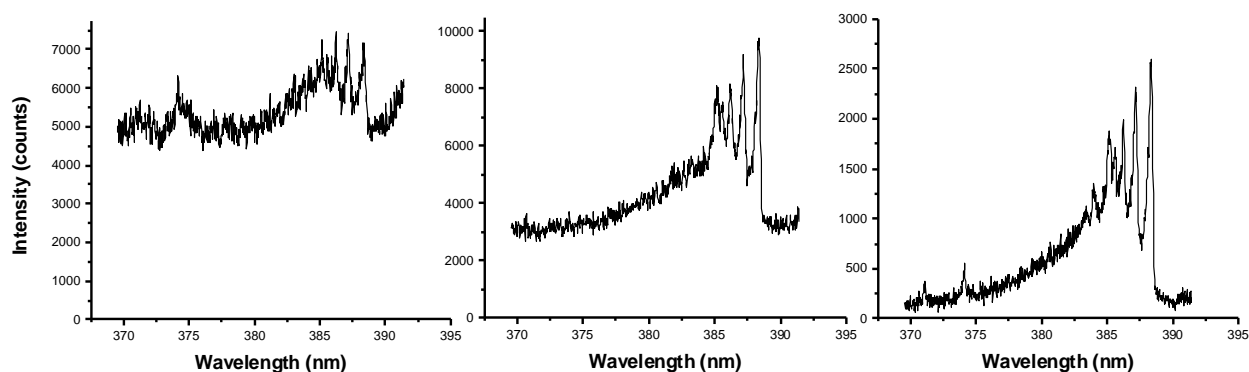


Figure 6. Benzoic acid spectra taken simultaneously with images in Figure 5. Gate delays and widths are as in Fig. 5.

References

- [1] Baudelet M, Guyon L, Yu J, Wolf J, Amodeo T, Frejafon E, and Laloi P 2006 *Applied Physics Letters* **88** 063901; Boueri M, Baudelet M, Yu J, Mao X, Mao S, and Russo R 2009 *Applied Surface Science* **255** 9566; St-Onge L, Sing R, Bechard S, and Sabsabi M 1999 *Applied Physics A-Materials Science & Processing* **69** S913
- [2] Grégoire S, Motto-Ros V, Ma Q, Lei W, Wang X, Pelascini F, Surma F, Detalle V, and Yu J 2012 *Spectrochimica Acta Part B: Atomic Spectroscopy* **74–75** 31